Results in Applied Mathematics 13 (2022) 100229

Contents lists available at ScienceDirect

Results in Applied Mathematics

journal homepage: www.elsevier.com/locate/results-in-applied-mathematics

Novel numerical techniques based on mimetic finite difference method for pricing two dimensional options

David Sena Attipoe [a,b], Antoine Tambue [c,*]

[a] The African Institute for Mathematical Sciences (AIMS), 6-8 Melrose Road, Muizenberg 7945, South Africa
[b] Department of Mathematics and Applied Mathematics, University of Cape Town, 7701 Rondebosch, South Africa
[c] Department of Computer science, Electrical engineering and Mathematical sciences, Western Norway University of Applied Sciences, Inndalsveien 28, 5063 Bergen, Norway,

ARTICLE INFO

Article history:
Received 23 September 2021
Received in revised form 20 November 2021
Accepted 24 November 2021
Available online 20 December 2021

Keywords:
Option pricing
European option
American option
Mimetic finite difference method
Fitted scheme

ABSTRACT

The Black–Scholes differential operator which underlies the option pricing of European and American options is known to be degenerate close to the boundary at zero. At this singularity, important properties of the differential operator are lost and the classical finite difference scheme applied to this problem fails to give accurate approximations as it is no longer monotone. In this paper novel numerical techniques based on mimetic finite difference method are proposed for accurately pricing European and American options. More precisely, we propose the mimetic and fitted mimetic finite difference methods, which are techniques that preserve and conserve general properties of the continuum operator in the discrete case. The fitted method further handles the degeneracy of the underlying partial differential equations (PDE). Those spatial discretization methods are coupled with the Euler implicit method for time discretization. Several numerical simulations are performed to demonstrate the robustness of our methods comparing to standard fitted finite volume method for both European and American put options.

1. Introduction

For many decades, the financial industry has seen a surge in the valuation of derivative securities. One such derivative security is an option, which is essentially a financial contract (traded) that renders to its owner the non-obligatory right to buy (call) or sell (put) a specified quantity of underlying assets at a fixed price (strike price) on (European option) or before (American option) a given date (maturity/expiry date). A closed form solution was obtained by Black and Scholes (1972) for the value of European option (V) with constant coefficients [1–3]. They showed that the value V is governed by the following second order parabolic differential equation with respect to time (t) and the price of the underlying stocks (x, y)

$$\frac{\partial V}{\partial t} + \frac{1}{2}\sigma_1^2 x^2 \frac{\partial^2 V}{\partial x^2} + \frac{1}{2}\sigma_2^2 y^2 \frac{\partial^2 V}{\partial y^2} + \rho\sigma_1\sigma_2 xy \frac{\partial^2 u}{\partial x \partial y} + r\left(x\frac{\partial V}{\partial x} + y\frac{\partial V}{\partial y}\right) - rV(x, y, t) = 0, \tag{1}$$

where σ_1, σ_2 are the volatilities associated to the stock prices x and y, respectively, ρ is the correlation coefficient between the two stocks and r is the interest rate.

Pricing the American option however requires that at each time step we determine both the value of the option and whether or not it is optimal to exercise at that value[1] (see [4]). This makes the valuation of an American option a free

* Corresponding author.
E-mail addresses: davida@aims.ac.za (D.S. Attipoe), antonio@aims.ac.za (A. Tambue).

[1] This is known as the early exercise constraint.

https://doi.org/10.1016/j.rinam.2021.100229

boundary problem [4]. American options are known to be governed by a linear complementarity problem (LCP) involving the Black–Scholes differential operator and a constraint on the value of the option (see [4–7]). The LCP fully encapsulates the finance reasoning behind American options to a system of partial differential inequalities (PDIs) under appropriate final and boundary conditions. There is however a challenge when solving PDIs since we have to deal with the free and moving boundary. A penalty approach was proposed, [4,8] to overcome this challenge by adding a small and continuous penalty term that converts the PDIs to a partial differential equation (PDE) under appropriate final and boundary conditions. Unlike PDIs, there are several tools for solving PDEs and these tools have strong theoretical backgrounds. It is therefore preferable to consider converting the PDIs to a PDE. The solution of the resulting penalized PDE is known to converge to that of the original problem (LCP) for both single and two assets American put option (see [4,8,9]).

However, there is, in general, no analytical solution to the resulting penalized PDE and hence numerical methods are the only tools used to provide realistic approximations. The commonly used standard discretization technique is the finite difference method (FDM) [5,10]. The underlying Black–Scholes differential operator is known to be degenerate at the boundary when the stock price equals zero [11]. At this singularity, important properties of the PDE are lost. A negative consequence here is that the classical finite difference scheme applied to such problems is no longer monotone and hence fails to give an accurate approximation when the stock price is small. Therefore, more sophisticated techniques that are adapted to handle the degeneracy must be sought. Moreover, when the stock price S is equal to the strike price K, the initial condition of the PDE has a discontinuity in its first derivative. This fact has a negative impact on the accuracy especially when the standard finite difference or standard upwind finite difference are used (see [5, chapter 26]). Therefore, for the spatial discretization of penalized PDE, it is suitable to construct methods that handle the degeneracy at both $X, Y = 0$ and the discontinuity at $X, Y = K$. In [12], a fitted finite volume technique for the one-dimensional Black–Scholes PDE was proposed to solve the previous drawback. Although this method was stable, it is only first order with respect to asset price variables. In [11] fitted numerical method based on mimetic for the one-dimensional Black–Scholes PDE was proposed and analyzed. The scheme has been proved to be very accurate comparing the finite difference method and the standard fitted finite volume for Europeans options. However the extension of the scheme in high dimension is not straightforward as the diffusion part of the Black Scholes operator has a full degenerate matrix. Furthermore the American options[2] have not been investigated.

The goal of this paper is to extend the work in [11] in high dimension for both European and American options. Comparing to [11], the contribution of this article can be summarized as follows

- Here we develop mimetic finite difference and fitted mimetic finite difference schemes for both Europeans and American options pricing in high dimension.[3]
- We provide several numerical simulations to demonstrate the robustness of our methods comparing to standard fitted finite volume method for both European and American put options.

The paper is organized as follows. In Section 2, we present briefly, the theoretical foundations for the paper. Further in the section, we present the support operator method upon which the mimetic finite difference methods are based for the penalized Black–Scholes PDE. In Section 3, we present our spatial discretization methods based on Mimetic finite difference method (MFD) and Fitted Mimetic finite difference (FMFD) to discretize the diffusion term of the Black Scholes PDE. Also in this section, we apply the so-called upwind-finite difference method to the convection term. We provide the full discretization of our two schemes with the standard implicit time stepping scheme. In Section 4, we present some numerical experiments to show the accuracy of the novel schemes compared to the fitted finite volume method presented in [12,13] for the two dimensional problems (European and American put options). A short summary of our funding is given in Section 5.

2. Theoretical framework

We present the following standard notations which we use in this paper. For $\Omega \subset \mathbb{R}^2$ and $1 \leq p < \infty$, we have $L^p(\Omega) = \{v : \left(\int_\Omega |v(x)|^p dx\right)^{1/p} < \infty\}$ is the space of all p-power Lebesgue measurable functions on Ω with the usual modification of $p = \infty$, where $v : \Omega \to \mathbb{R}$ is seen as an equivalence class of such measurable functions. Then the inner product for $L^2(\Omega)$ is denoted by $(\cdot, \cdot)$. We equip $L^p(\Omega)$ with the norm $\|\cdot\|_{0,p}$. Now for $l = 0, 1, 2, \ldots$, we let W_p^l be the Sobolev space with norm $\|\cdot\|_{l,p}$ and semi-norm $|\cdot|_{l,p}$. Then for the special case of $p = 2$, we denote by $H^l(\Omega)$ the associated Sobolev space with the corresponding norm $\|\cdot\|_l$. We denote $H_0^l(\Omega) = \{v \in H^l(\Omega) : Tv = v|_{\partial\Omega} = 0\}$, where $T : H^l(\Omega) \to L^p(\partial\Omega)$ is the trace operator. Now for any Hilbert space $H(\Omega)$ of classes of functions defined on Ω, we denote by $L^p((0,T); H(\Omega))$ the space defined by

$$L^p((0,T); H(\Omega)) = \{v(\cdot,t) : v(\cdot,t) \in H(\Omega)\ a.e \text{ in } (0,T) : \|v(\cdot,t)\|_H \in L^p((0,T))\} \tag{2}$$

which is equipped with the norm

$$\|v\|_{L^p((0,T);H(\Omega))} = \left(\int_0^T \|v(\cdot,t)\|_H^p dt\right)^{1/p}$$

[2] The more challenge case where no analytical solution is available even for constant coefficients.

[3] Here we focus on dimension 2 as the same idea can easily be used in dimension $d > 2$.

where $\|\cdot\|_H$ is the natural norm on $H(\Omega)$. Since (1) is known to be degenerate, we introduce a weighted inner product on $(L^2(\Omega))^2$ by $(\mathbf{u},\mathbf{v})_w := \int_\Omega (x^2u_1v_1 + y^2u_2v_2)d\Omega$, for any $\mathbf{u} = (u_1, u_2)^T$ and $\mathbf{v} = (v_1, v_2)^T \in (L^2_w(\Omega))^2$. The corresponding weighted L^2-norm is given by

$$\|\mathbf{v}\|_{0,w} := \sqrt{(\mathbf{v},\mathbf{v})_w} = \left(\int_\Omega (x^2v_1^2 + y^2v_2^2)d\Omega\right)^{1/2}.$$

Hence the space of all weighted square-integrable functions is defined as

$$\mathbf{L}^2_w(\Omega) := \{\mathbf{v} \in (L^2(\Omega))^2 : \|\mathbf{v}\|_{0,w} < \infty\}.$$

It is very clear with the use of standard arguments that the pair $(\mathbf{L}^2_w(\Omega), (\cdot,\cdot)_w)$ is a Hilbert space (cf., for example [14]). Then we can finally define the following weighted Sobolev space

$$H^1_{0,w}(\Omega) := \left\{v : v \in L^2(\Omega), \nabla v \in \mathbf{L}^2_w(\Omega) \text{ and } v|_{\partial\Omega_D} = 0\right\},$$

where $\partial\Omega_D$ is the Dirichlet boundary condition part of $\partial\Omega$. Then we define the weighted inner product on $H^1_{0,w}(\Omega)$ by $(\cdot,\cdot)_H := (\cdot,\cdot) + (\cdot,\cdot)_w$, which is equipped with the norm

$$\|v\|_{1,w} = \left[\|v\|_0^2 + \|\nabla v\|^2_{0,w}\right]^{1/2}.$$

2.1. The continuous problem

In this subsection, we provide the linear complementarity problem (LCP), for two underlying assets (x, y), which is well known to govern American put options [4,8]. For $V(x, y, t)$, the LCP is given by

$$\begin{cases} \mathcal{L}V\,(V(x,y,t) - V^*(x,y)) = 0, \quad a.e.\ in\ \ \Omega\times(0,T) \\ V(x,y,t) - V^*(x,y) \geq 0, \quad a.e.\ in\ \ \Omega\times(0,T) \\ \mathcal{L}V \geq 0, \quad a.e.\ in\ \ \Omega\times(0,T) \end{cases} \tag{3}$$

where V^* is the payoff function which is defined as

$$V^*(x,y) = \max\left(K - (\alpha_1 x + \alpha_2 y), 0\right),$$

and K is the agreed strike price at expiry date T, and

$$\mathcal{L}V = -\frac{\partial V}{\partial t} - \frac{1}{2}\sigma_1^2x^2\frac{\partial^2V}{\partial x^2} - \frac{1}{2}\sigma_2^2y^2\frac{\partial^2V}{\partial y^2} - \rho\sigma_1\sigma_2xy\frac{\partial^2u}{\partial x\partial y} - r\left(x\frac{\partial V}{\partial x} + y\frac{\partial V}{\partial y}\right) + rV(x,y,t), \tag{4}$$

where $\Omega = (0, X)\times(0, Y)$, is the truncated domain, r is the interest rate, and α_1, α_2 are the weights associated to the assets x and y, respectively. The boundary conditions and the final condition are given by

$$\begin{aligned} &V(0,y,t) = g_1(y,t), \quad y\in(0,Y), t\in[0,T], \\ &V(x,0,t) = g_2(x,t), \quad x\in(0,X), t\in[0,T], \\ &\quad V(X,y,t) = 0, \quad V(x,Y,t) = 0 \end{aligned} \tag{5}$$

$$V(x,y,T) = V^*(x,y). \tag{6}$$

The functions g_1 and g_2 are given and provide suitable boundary conditions. Typically, we determine $g_1(\cdot,\cdot)$ by solving the one-dimensional American put option problem.

2.1.1. Reformulated problem

In [4,8] the LCP was reformulated for convenience during theoretical analysis. We write the LCP in conservative form to facilitate the theoretical analysis into a variational form. The variational forms have been extensively studied in [15]. The well-posedness here is studied in a truncated domain $\Omega = [0, X]\times[0, Y]$, where we have assumed that $X \gg K$ and $Y \gg K$ [8,15]. Let V_0 be a twice differentiable function satisfying the boundary and final conditions in (5)–(6). Using the transformation

$$u(x,y,t) = e^{\beta t}\left(V_0 - V\right), \tag{7}$$

the problem (3) then becomes

$$\begin{cases} Lu(x,y,t) \leq f, \\ u(x,y,t) - u^*(x,y,t) \leq 0, \\ (Lu - f)\,(u(x,y,t) - u^*(x,y,t)) = 0, \end{cases} \tag{8}$$

where L is the conservative differential operator given by

$$Lu = -u_t - \nabla\cdot(K\nabla u + \mathbf{b}u) + cu = f(u), \tag{9}$$

with

$$K = \begin{pmatrix} k_{11} & k_{12} \\ k_{21} & k_{22} \end{pmatrix} = \begin{pmatrix} \frac{1}{2}\sigma_1^2 x^2 & \frac{1}{2}\rho\sigma_1\sigma_2 xy \\ \frac{1}{2}\rho\sigma_1\sigma_2 xy & \frac{1}{2}\sigma_2^2 y^2 \end{pmatrix} = \begin{pmatrix} k_{11} & 0 \\ 0 & k_{22} \end{pmatrix} + \begin{pmatrix} 0 & k_{12} \\ k_{21} & 0 \end{pmatrix} = K_1 + K_2,$$

$$\mathbf{b} = \begin{pmatrix} b_1 \\ b_2 \end{pmatrix} = \begin{pmatrix} rx - \sigma_1^2 x - \frac{1}{2}\rho\sigma_1\sigma_2 x \\ ry - \sigma_2^2 y - \frac{1}{2}\rho\sigma_1\sigma_2 y \end{pmatrix}, c = 3r - (\sigma_1^2 + \sigma_2^2 + \rho\sigma_1\sigma_2), \text{ and } \beta := \sigma_1^2$$

and

$$f(x, y, t) = e^{\beta t}\mathcal{L}V_0, \quad u^* = e^{\beta t}\left(V_0 - V^*\right),$$

with boundary and final conditions

$$\begin{aligned} &u(0, y, t) = 0 = u(X, y, t), \quad \text{for all } t \in [0, T], \quad y \in [0, Y], \\ &u(x, 0, t) = 0 = u(x, Y, t), \quad \text{for all } t \in [0, T], \quad x \in [0, X]. \end{aligned}$$

and

$$u(x, y, T) = u^*(x, y, T).$$

Note that any positive constant may be used for β.

2.1.2. Power penalty method

Now by adding a penalty term to the LCP (3) yields

$$\mathcal{L}V_\lambda + \lambda\left[V^* - V_\lambda\right]_+^{1/k} = 0 \tag{10}$$

with (5)–(6), or

$$Lu_\lambda + \lambda\left[u^* - u_\lambda\right]_+^{1/k} = f(x, y, t), \quad (x, y) \in \Omega \tag{11}$$

with boundary and final conditions

$$\begin{aligned} &u_\lambda(0, y, t) = 0 = u_\lambda(X, y, t), \quad t \in [0, T], \quad y \in [0, Y], \\ &u_\lambda(x, 0, t) = 0 = u_\lambda(x, Y, t), \quad t \in [0, T], \quad x \in [0, X] \\ &u_\lambda(x, y, T) = u^*(x, y, T). \end{aligned}$$

Where in (11), u_λ is the penalized solution of the reformulated problem, V_λ is the penalized solution in (3), $k > 0$ is the power of the penalty term and $\lambda > 1$ is the penalty parameter. When $k = \frac{1}{2}$, the penalty approach corresponds to a quadratic penalty approach. The case for $k = 1$ is however standard in literature. For $k > 1$, we have the so-called lower-order penalty approach [4,8]. Using the same arguments as in [4,8], (11) is well-posed.

Theorem 1. *Suppose that [4, Assumption 2.13] and the assumptions in [4, Lemma 2.9] are fulfilled. Then, there exists a constant $C > 0$, independent of u, u_λ, λ such that*

$$\|u - u_\lambda\|_{L^\infty(0,T;L^2(\Omega))} + \|u - u_\lambda\|_{L^2(0,T;H^1_{0,\omega}(\Omega))} \leq \frac{C}{\lambda^{k/2}}, \tag{12}$$

where k is the power penalty using in (11).

Proof. The proof can be found [4,8]. □

Remark 1. It is important to note here that, without loss of generality, we are only considering the simplest model where the coefficients are constant. Furthermore, note that (10) becomes (1) with $\lambda = 0$, which is the Black–Scholes equation for the European option. In the sequel of this paper, we will replace u_λ by u to ease the notation.

2.2. Support operator method

Details on characterization and motivation of mimetic finite difference method can be found in [11,16–19]. Now, for the purposes of an illustration, we reconsider as in [11] the following diffusion equation

$$-\nabla\cdot(\mathbf{K}\nabla u(x, y)) = f, \quad (x, y) \in \Omega \subset \mathbb{R}^2 \tag{13}$$

with boundary condition

$$u(x, y) = 0, \quad (x, y) \in \partial\Omega,$$

where $\mathbf{K} > 0$ is a bounded invertible matrix function of (x, y)[4] and f could be a forcing function. Then we define an operator $\mathbf{A} : H \to H$, by

$$\mathbf{A}u = -\nabla \cdot (\mathbf{K}\nabla u(x, y)), \quad (x, y) \in \Omega \tag{14}$$

with properties

$$(\mathbf{A}u, v)_H = (u, \mathbf{A}v)_H, \quad (\mathbf{A}u, u)_H > 0, \quad \mathbf{F} = f. \tag{15}$$

That is (13) becomes

$$\mathbf{A}u = \mathbf{F}. \tag{16}$$

Then (13) can be rewritten as the following first-order system

$$\begin{cases} \nabla \cdot \mathbf{w} = \mathbf{F} \\ \mathbf{w} = -K\nabla u, \end{cases} \tag{17}$$

which is equivalent to

$$\mathbf{w} - \mathbf{G}u = 0, \ \mathbf{D}\mathbf{w} = \mathbf{F}, \tag{18}$$

where the operators $\mathbf{G}$ and $\mathbf{D}$ are defined as

$$\begin{cases} \mathbf{G}u = -\mathbf{K}\nabla u \ \text{ on } \ \Omega \\ \mathbf{D}\mathbf{w} = \nabla \cdot \mathbf{w} \ \text{ on } \ \Omega \\ \mathbf{A} = \mathbf{D}\mathbf{G} \end{cases} \tag{19}$$

Let $H = L^2(\Omega)$ be the space of scalar functions u that are smooth on the Ω equipped with inner product

$$(u, v)_H = \int_\Omega uv d\Omega, \quad u, v \in H, \tag{20}$$

and $\mathbf{H} = \left(L^2(\Omega)\right)^2$ equipped with inner product

$$(\mathbf{w}, \mathbf{z})_{\mathbf{H}} = \int_\Omega (\mathbf{K}^{-1}\mathbf{w}, \mathbf{z}) d\Omega, \quad \mathbf{w}, \mathbf{z} \in \mathbf{H} = \left(L^2(\Omega)\right)^2. \tag{21}$$

The inner product (21) is weighted by the inverse of $\mathbf{K}$. Thus, $(\cdot, \cdot)$ is the standard inner product of $\mathbb{R}^2$. Note that the following properties are fulfilled [19–21]

$$(\mathbf{D}\mathbf{w}, u)_H = (\mathbf{w}, \mathbf{G}u)_{\mathbf{H}} \tag{22}$$

$$(\mathbf{D}\mathbf{w}, 1)_H = 0, \tag{23}$$

where 1 is the constant function with value 1. The properties (22)–(23) are the important properties of the continuum operators that we want our discrete operators in the next section to mimic.

3. Mimetic finite difference and fitted-mimetic finite difference methods for options pricing

Let us first build a mimetic finite difference method to discretize the diffusion part of our continuous problem (11). As we mentioned earlier, the corresponding discrete operators will mimic the properties (22)–(23). In general, the mimetic methods are applied on unstructured meshes [22]. Here a rectangular mesh will be used and without loss of generality, the domain $\Omega = [0, X] \times [0, Y]$ is divided into $(N_x + 1) \times (N_y + 1)$ non-overlapping intervals $\mathcal{T} = (I_i \times I_j)_{0 \le i \le Nx+1, 0 \le i \le Ny+1}$, such that $I_i = (x_i, x_{i+1}), \ i = 0, 1, \ldots, N_x$, with $0 = x_0 < x_1 < \cdots < x_{N_x+1} = X$ and $I_j = (y_j, y_{j+1}), \ j = 0, 1, \ldots, N_y$, with $0 = y_0 < y_1 < \cdots < y_{N_y+1} = Y$. We set $h_{x_i} = x_{i+1} - x_i$, with $h_x = \max_{0 \le i \le (N_x+1)} h_{x_i}$ and $h_{y_j} = y_{j+1} - y_j$, with $h_y = \max_{0 \le j \le (N_y+1)} h_{y_j}$.

Now, we define the following mid-points $x_{i-\frac{1}{2}} = \dfrac{x_i + x_{i-1}}{2}$, $x_{i+\frac{1}{2}} = \dfrac{x_i + x_{i+1}}{2}$ for $i = 1, \ldots, N_x$, $y_{j-\frac{1}{2}} = \dfrac{y_j + y_{j-1}}{2}$ and $y_{j+\frac{1}{2}} = \dfrac{y_j + y_{j+1}}{2}$ for $j = 1, \ldots, N_y$. We also set $x_{-\frac{1}{2}} = x_0$, $x_{N_x+\frac{3}{2}} = x_{N_x+1}$, $y_{-\frac{1}{2}} = y_0$ and $y_{N_y+\frac{3}{2}} = y_{N_y+1}$. Now for $i = 0, 1, \ldots, N_x + 1$, we set $l_{x_i} = x_{i+1/2} - x_{i-1/2}$, $l_x = \max_{0 \le i \le (N_x+1)} l_{x_i}$. We also set $l_{y_j} = y_{j+1/2} - y_{j-1/2}$ for $j = 0, 1, \ldots, N_y + 1$, $l_y = \max_{0 \le j \le (N_y+1)} l_{y_j}$. Furthermore, we set $x_{-\frac{1}{2}} = x_0$ and $x_{N_x+\frac{3}{2}} = x_{N_x+1}$.[5] Similarly, $y_{-\frac{1}{2}} = y_0$ and $y_{N_y+\frac{3}{2}} = y_{N_y+1}$.[6] Note the family $(\Omega_i \times \Omega_j)_{0 \le i \le Nx+1, 0 \le i \le Ny+1}$ is another partition of Ω with $\Omega_i = (x_{i-\frac{1}{2}}, x_{i+\frac{1}{2}})$ and $\Omega_j = (y_{j-\frac{1}{2}}, y_{j+\frac{1}{2}})$. We will call this the dual partition of the family $(I_i \times I_j)_{0 \le i \le Nx+1, 0 \le i \le Ny+1}$ (see Fig. 1).

4 A material property tensor in engineering sciences.

5 Function evaluation at $x_{-\frac{1}{2}}$ or $x_{N_x+\frac{3}{2}}$ is understood as evaluation at $x_0 = 0$ or at $x_{N_x+1} = X$.

6 Function evaluation at $y_{-\frac{1}{2}}$ or $y_{N_y+\frac{3}{2}}$ is understood as evaluation at $y_0 = 0$ or at $y_{N_y+1} = Y$.

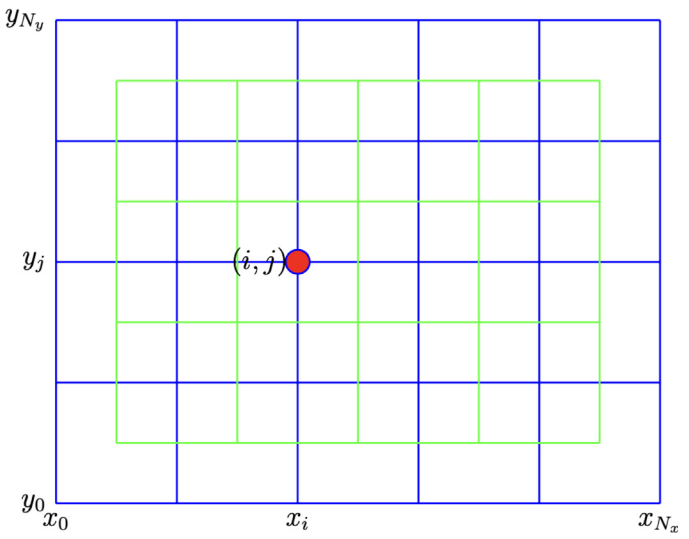

Fig. 1. Fitted mimetic grid $\mathcal{T}$ in blue and its dual partition in green.

3.1. Discrete inner products

We define discrete analogs of the two continuous inner products (20) and (21) which use a quadrature rule on each cell to approximate the integrals. Let *HC* and **HC** denote the discrete spaces of discrete scalar and vector functions for $H = L^2(\Omega)$ and $\mathbf{H} = (L^2(\Omega))^2$ respectively, in the partition $\mathcal{T}$. Then the discrete L^2 norm defined in *HC* is given by

$$(U, V)_{HC} = \sum_{i=0}^{N_x+1} \sum_{j=0}^{N_y+1} l_{x_i} l_{y_j} U_{i,j} V_{i,j}. \tag{24}$$

Since the discrete information for fluxes are located at the cell centers, we adopt the midpoint rule for the inner product (21). Let the cartesian components of the tensor $\mathbf{K}$ be given by K_{xx}, $K_{xy} = K_{yx}$, K_{yy}. Then, $(\mathbf{K}^{-1})_{xx}$, $(\mathbf{K}^{-1})_{xy} = (\mathbf{K}^{-1})_{yx}$, $(\mathbf{K}^{-1})_{yy}$ are the associated cartesian components of the tensor $\mathbf{K}^{-1}$, the inverse of $\mathbf{K}$. For any vectors, $\mathbf{W}, \mathbf{Z}$, we represent their components as $\mathbf{W} = (W_x, W_y)$ and $\mathbf{Z} = (Z_x, Z_y)$.

$$\left(\mathbf{K}^{-1}\mathbf{W}, \mathbf{Z}\right) = (\mathbf{K}^{-1})_{xx} W_x Z_x + (\mathbf{K}^{-1})_{yy} W_y Z_y. \tag{25}$$

For simplicity, we choose the following,

$$W_{x_{i+\frac{1}{2},j}} = W_{i+\frac{1}{2},j}, \;\; W_{y_{i,j+\frac{1}{2}}} = W_{i,j+\frac{1}{2}}, \; Z_{x_{i+\frac{1}{2},j}} = Z_{i+\frac{1}{2},j}, \;\; Z_{y_{i,j+\frac{1}{2}}} = Z_{i,j+\frac{1}{2}}.$$

The discrete $(L^2(\Omega))^2$ norm defined in **HC** is given by

$$(\mathbf{W}, \mathbf{Z})_{\mathbf{HC}} = \sum_{i=0}^{N_x+1} \sum_{j=0}^{N_y+1} h_{x_i} h_{y_j} \left[(\mathbf{K}_{xx}^{-1})_{i+\frac{1}{2},j} W_{i+\frac{1}{2},j} Z_{i+\frac{1}{2},j} + (\mathbf{K}_{yy}^{-1})_{i,j+\frac{1}{2}} W_{i,j+\frac{1}{2}} Z_{i,j+\frac{1}{2}} \right] \tag{26}$$

Note that in *HC* and **HC**, for the computation adjoint relationships and entries of matrices corresponding to the discrete operators, the following standard inner products are introduced

$$[U, V]_{HC} = \sum_{i=1}^{N_x} \sum_{j=1}^{N_y} U_{i,j} V_{i,j}, \qquad U, V \in HC, \tag{27}$$

$$[\mathbf{W}, \mathbf{Z}]_{\mathbf{HC}} = \sum_{i=1}^{N_x} \sum_{j=1}^{N_y} \left[W_{i+\frac{1}{2},j} Z_{i+\frac{1}{2},j} + W_{i,j+\frac{1}{2}} Z_{i,j+\frac{1}{2}} \right]. \tag{28}$$

We furthermore note that, in *HC* and **HC**, the two inner products are linked by

$$(U, V)_{HC} = [\mathcal{M}U, V]_{HC}, \qquad (W, Z)_{\mathbf{HC}} = [\mathcal{S}\mathbf{W}, \mathbf{Z}]_{\mathbf{HC}} \tag{29}$$

where $\mathcal{M}$ and $\mathcal{S}$ are coefficients, please see [20,21] for more information.

3.2. The discrete divergence and discrete flux

In this section, we present the discrete version of the divergence operator **D**. The resulting discrete divergence is denoted by $\mathcal{D}$. Then the discrete flux is given by

$$(\mathcal{D}W)_{i,j} = \left(\frac{W_{i+\frac{1}{2},j} - W_{i-\frac{1}{2},j}}{l_{x_i}} + \frac{W_{i,j+\frac{1}{2}} - W_{i,j-\frac{1}{2}}}{l_{y_j}} \right) \quad i = 0, 1, \ldots, N_x + 1, \quad j = 0, 1, \ldots, N_y + 1. \tag{30}$$

Then it is easy to check that

$$(\mathcal{D}W, 1)_{HC} = 0. \tag{31}$$

This is the divergence property of the discrete divergence $\mathcal{D}$ which mimics the continuous divergence in (23). Here we set $\mathbf{G} = -\mathbf{K}\nabla$ with $\mathbf{K} = \begin{pmatrix} k_{11} & 0 \\ 0 & k_{22} \end{pmatrix}$, a 2×2 diagonal matrix tensor. In this case therefore, $\mathbf{K}^{-1} = \begin{pmatrix} \frac{1}{k_{11}} & 0 \\ 0 & \frac{1}{k_{22}} \end{pmatrix}$. Now, we determine the discrete version of **G** denoted by $\mathcal{G}$ that mimics the continuous version of the properties we have already mentioned. In fact, $\mathcal{G}$ should satisfy the following property

$$(\mathcal{D}W, U)_{HC} = (W, \mathcal{G}U)_{\mathbf{HC}}. \tag{32}$$

We then expand (32) as below,

$$\begin{aligned} \sum_{i=0}^{N_x+1} \sum_{j=0}^{N_y+1} U_{i,j} (\mathcal{D}W)_{i,j} l_{x_i} l_{y_j} = & \sum_{i=0}^{N_x+1} \sum_{j=0}^{N_y+1} \left(K^{-1}_{xx_{i+\frac{1}{2},j}} W_{i,j+\frac{1}{2}} W_{i+\frac{1}{2},j} (\mathcal{G}U)_{i+\frac{1}{2},j} \right) \\ & + \sum_{i=0}^{N_x+1} \sum_{j=0}^{N_y+1} \left(K^{-1}_{yy_{i,j+\frac{1}{2}}} W_{i,j+\frac{1}{2}} (\mathcal{G}U)_{i,j+\frac{1}{2}} \right) h_{x_i} h_{y_j}. \end{aligned} \tag{33}$$

Which then leads to

$$\begin{aligned} & \sum_{i=0}^{N_x+1} \sum_{j=0}^{N_y+1} U_{i,j} \left\{ \left(\frac{W_{i+\frac{1}{2},j} - W_{i-\frac{1}{2},j}}{l_{x_i}} + \frac{W_{i,j+\frac{1}{2}} - W_{i,j-\frac{1}{2}}}{l_{y_j}} \right) \right\} l_{x_i} l_{y_j} \\ & = \sum_{i=0}^{N_x+1} \sum_{j=0}^{N_y+1} \left(K^{-1}_{xx_{i+\frac{1}{2},j}} W_{i+\frac{1}{2},j} (\mathcal{G}U)_{i+\frac{1}{2},j} + K^{-1}_{yy_{i,j+\frac{1}{2}}} W_{i,j+\frac{1}{2}} (\mathcal{G}U)_{i,j+\frac{1}{2}} \right) h_{x_i} h_{y_j}. \end{aligned} \tag{34}$$

Then grouping the terms of (34), we have,

$$\begin{aligned} & \sum_{i=0}^{N_x+1} \sum_{j=0}^{N_y+1} \left[l_{y_j} U_{i,j} - K^{-1}_{xx_{i+\frac{1}{2},j}} h_{x_i} h_{y_j} (\mathcal{G}U)_{i+\frac{1}{2},j} \right] W_{i+\frac{1}{2},j} - \sum_{i=0}^{N_x+1} \sum_{j=0}^{N_y+1} l_{y_j} U_{i,j} W_{i-\frac{1}{2},j} + \\ & \sum_{i=0}^{N_x+1} \sum_{j=0}^{N_y+1} \left[l_{x_i} U_{i,j} - K^{-1}_{yy_{i,j+\frac{1}{2}}} h_{x_i} h_{y_j} (\mathcal{G}U)_{i,j+\frac{1}{2}} \right] W_{i,j+\frac{1}{2}} - \sum_{i=0}^{N_x+1} \sum_{j=0}^{N_y+1} l_{x_i} U_{i,j} W_{i,j-\frac{1}{2}} = 0. \end{aligned} \tag{35}$$

Then we can rewrite the terms as follows

$$\begin{aligned} & \sum_{i=0}^{N_x+1} \sum_{j=0}^{N_y+1} \left[l_{y_j} U_{i,j} - K^{-1}_{xx_{i+\frac{1}{2},j}} h_{x_i} h_{y_j} (\mathcal{G}U)_{i+\frac{1}{2},j} \right] W_{i+\frac{1}{2},j} - \sum_{i=1}^{N_x+1} \sum_{j=0}^{N_y+1} l_{y_j} U_{i,j} W_{i-\frac{1}{2},j} \\ & - \sum_{j=0}^{N_y+1} l_{y_j} U_{0,j} W_{-\frac{1}{2},j} + \sum_{i=0}^{N_x+1} \sum_{j=0}^{N_y+1} \left[l_{x_i} U_{i,j} - K^{-1}_{yy_{i,j+\frac{1}{2}}} h_{x_i} h_{y_j} (\mathcal{G}U)_{i,j+\frac{1}{2}} \right] W_{i,j+\frac{1}{2}} \\ & - \sum_{i=0}^{N_x+1} \sum_{j=1}^{N_y+1} l_{x_i} U_{i,j} W_{i,j-\frac{1}{2}} - \sum_{i=0}^{N_x+1} l_{x_i} U_{i,0} W_{i,-\frac{1}{2}} = 0. \end{aligned} \tag{36}$$

Now, re-indexing any terms with $i-\frac{1}{2}$ to $i+\frac{1}{2}$, and $j-\frac{1}{2}$ to $j+\frac{1}{2}$, and making using of the fact that $h_{N_x}=0$ and $h_{N_y}=0$, then (36) becomes

$$\begin{aligned}
&\sum_{i=0}^{N_x}\sum_{j=0}^{N_y+1}\left[-l_{y_j}(U_{i+1,j}-U_{i,j})-K^{-1}_{xx_{i+\frac{1}{2},j}}h_{x_i}h_{y_j}(\mathcal{G}U)_{i+\frac{1}{2},j}\right]W_{i+\frac{1}{2},j}-\sum_{j=0}^{N_y+1}l_{y_j}U_{0,j}W_{-\frac{1}{2},j}\\
&+\sum_{i=0}^{N_x+1}\sum_{j=0}^{N_y}\left[-l_{x_i}(U_{i,j+1}-U_{i,j})-K^{-1}_{yy_{i,j+\frac{1}{2}}}h_{x_i}h_{y_j}(\mathcal{G}U)_{i,j+\frac{1}{2}}\right]W_{i,j+\frac{1}{2}}-\sum_{i=0}^{N_x+1}l_{x_i}U_{i,0}W_{i,-\frac{1}{2}}\\
&+\sum_{j=0}^{N_y+1}l_{y_j}U_{N_x+1,j}W_{N_x+\frac{3}{2},j}+\sum_{i=0}^{N_x+1}l_{x_i}U_{i,N_y+1}W_{i,N_y+\frac{3}{2}}=0.
\end{aligned}\tag{37}$$

This technique is done to fully concentrate the fluxes at the (i,j)thnode to enhance the mimicking property at that node. We further note here that, (37) holds for all U in HC such that $U_{0,j}=U_{N_x+1,j}=0$ and $U_{i,0}=U_{i,N_y+1}=0$. Hence solving for $(\mathcal{G}U)_{i+1/2,j}$ gives

$$(\mathcal{G}U)_{i+\frac{1}{2},j}=-\left(\left[\frac{l_{y_j}k_{11_{i+\frac{1}{2}}}}{h_{x_i}h_{y_j}}\right]\right)\left(U_{i+1,j}-U_{i,j}\right);\qquad i=0,\dots,N_x,\ \ j=0,\dots,N_y+1.\tag{38}$$

and solving for $(\mathcal{G}U)_{i,j+1/2}$,

$$(\mathcal{G}U)_{i,j+\frac{1}{2}}=-\left(\left[\frac{l_{x_i}k_{22_{j+\frac{1}{2}}}}{h_{y_j}h_{x_i}}\right]\right)\left(U_{i,j+1}-U_{i,j}\right),\qquad i=1,\dots,N_x,j=1,\dots,N_y+1.\tag{39}$$

Let $\mathcal{A}_h$ be the discrete diffusion operator obtained by forming the composition of the discrete divergence and gradient operator $\mathcal{D}$ and $\mathcal{G}$ respectively. This by construction, $\mathcal{D}:\mathbf{HC}\to HC$ and $\mathcal{G}:HC\to\mathbf{HC}$ is given by $\widehat{\mathcal{A}_h}:HC\to HC$.

3.3. Mimetic finite difference scheme for penalized American option

In this section, we aim to discretize penalized American option problem (11). The mimetic finite difference method will be used for the diagonalized diffusion term (see $\mathbf{K}_1$ below), while the central difference is used to approximate the other diffusion term (see $\mathbf{K}_2$ below), and the first order upwind-finite difference scheme for the convection terms. Remember that for simplicity we have set $u_\lambda=u$, then we have

$$\begin{cases}
-\dfrac{\partial u}{\partial t}+\mathbf{D}w-\nabla\cdot[\mathbf{K}_2\nabla u+\mathbf{b}u]+cu+\lambda[u^*-u]_+^{1/k}=f(x,y,t)\\
\qquad\qquad\mathbf{G}u:=w=-\mathbf{K}_1\nabla u\\
\qquad\qquad\mathbf{A}=\mathbf{DG},
\end{cases}\tag{40}$$

where

$$\mathbf{K}_1=\begin{pmatrix}k_{11}&0\\0&k_{22}\end{pmatrix}=\begin{pmatrix}\frac{1}{2}\sigma_1^2x^2&0\\0&\frac{1}{2}\sigma_2^2y^2\end{pmatrix},\quad \mathbf{K}_2=\begin{pmatrix}0&k_{12}\\k_{21}&0\end{pmatrix}=\begin{pmatrix}0&\frac{1}{2}\rho\sigma_1\sigma_2xy\\\frac{1}{2}\rho_{12}\sigma_1\sigma_2xy&0\end{pmatrix},$$
$$\mathbf{b}=\begin{pmatrix}b_1x\\b_2y\end{pmatrix}=\begin{pmatrix}(r-\sigma_1^2-\frac{1}{2}\rho\sigma_1\sigma_2)x\\(r-\sigma_2^2-\frac{1}{2}\rho\sigma_1\sigma_2)y\end{pmatrix},\ c=3r-(\sigma_1^2+\sigma_2^2+\rho\sigma_1\sigma_2).$$

We then partition $I_i:=(0,X)$ into N_x+1 and $I_j:=(0,Y)$ into N_y+1 subintervals respectively, with dual partitions as we did for the elliptic problems. Then we have that,

$$U_{i,j}\approx U(x_i,y_j,t),\ \ l_{x_i}=x_{i+1/2}-x_{i-1/2},\ \ l_{y_j}=y_{j+1/2}-y_{j-1/2},h_{x_i}=x_{i+1}-x_i,\ \ h_{y_j}=y_{j+1}-y_j,$$

for $i=0,1,\dots,N_x$ and $j=0,1,\dots,N_y$. Let us set $w_{i+\frac{1}{2},j}:=\dfrac{w_{i+1,j}-w_{i,j}}{2}$, $w_{i-\frac{1}{2},j}:=\dfrac{w_{i,j}-w_{i-1,j}}{2}$, $w_{i,j+\frac{1}{2}}:=\dfrac{w_{i,j+1}-w_{i,j}}{2}$, $w_{i,j-\frac{1}{2}}:=\dfrac{w_{i,j}-w_{i,j-1}}{2}$. We can easily see that $w_{i,j}\approx w(x_i,y_j,t)$, for $i=0,1,\dots,N_x$ and $j=0,1,\dots,N_y$.

That is the discrete mimetic operators (prime and derived) are given by

$$(Dw)_{i,j}=\frac{w_{i+\frac{1}{2},j}-w_{i-\frac{1}{2},j}}{l_{x_i}}+\frac{w_{i,j+\frac{1}{2}}-w_{i,j-\frac{1}{2}}}{l_{y_j}},\ \ i=0,\dots,N_x+1,\ \ j=0,\dots,N_y+1,\tag{41}$$

and

$$(\mathcal{G}U)_{i+\frac{1}{2},j}=-\left(\left[\frac{l_{y_j}k_{11_{i+\frac{1}{2}}}}{h_{x_i}h_{y_j}}\right]\right)\left(U_{i+1,j}-U_{i,j}\right),\ \ i=0,\dots,N_x,\ \ j=0,\dots,N_y+1,\tag{42}$$

$$(\mathcal{G}U)_{i,j+\frac{1}{2}} = -\left(\left[\frac{l_{x_i}k22_{j+\frac{1}{2}}}{h_{x_i}h_{y_j}}\right]\right)\left(U_{i,j+1}-U_{i,j}\right),\ i=0,\dots,N_x,\ j=0,\dots,N_y+1. \tag{43}$$

Now using this the following ordering for the grid, i.e. $z_{i,j} = (i-1)\times N_x + j$, for $i = 1,\dots,N_x$, and $j = 1,\dots,N_y$ we have that

$$U_h = (U_{1,1}, U_{1,2}, \dots, U_{1,N_y}, \dots, U_{N_x,1}, U_{N_x,2}, \dots, U_{N_x,N_y})^T. \tag{44}$$

Then the discrete operator $\widehat{\mathcal{A}}_h$ is given by

$$\begin{aligned}\widehat{\mathcal{A}}_h U_h[z_{i,j}] = (\mathcal{D}\mathcal{G}U)_h &= \frac{(\mathcal{G}U)_{i+\frac{1}{2},j} - (\mathcal{G}U)_{i-\frac{1}{2},j}}{l_{x_i}} + \frac{(\mathcal{G}U)_{i,j+\frac{1}{2}} - (\mathcal{G}U)_{i,j-\frac{1}{2}}}{l_{y_j}}\\ &= \frac{-\left(\frac{l_{y_j}k11_{i+\frac{1}{2}}}{h_{y_j}}\right)\frac{U_{i+1,j}-U_{i,j}}{h_{x_i}} + \left(\frac{l_{y_j}k11_{i-\frac{1}{2}}}{h_{y_j}}\right)\frac{U_{i,j}-U_{i-1,j}}{h_{x_{i-1}}}}{l_{x_i}}\\ &+ \frac{-\left(\frac{l_{x_i}k22_{j+\frac{1}{2}}}{h_{x_i}}\right)\frac{U_{i,j+1}-U_{i,j}}{h_{y_j}} + \left(\frac{l_{x_i}k22_{j-\frac{1}{2}}}{h_{x_i}}\right)\frac{U_{i,j}-U_{i,j-1}}{h_{y_{j-1}}}}{l_{y_j}}\end{aligned} \tag{45}$$

for $i = 1,\dots,N_x$, $j = 1,\dots,N_y$, or

$$\widehat{\mathcal{A}}_h U_h[z_{i,j}] = \alpha_{i,j}U_{i+1,j} + \beta_{i,j}U_{i,j+1} + \gamma_{i,j}U_{i,j} + \Gamma_{i,j}U_{i-1,j} + \delta_{i,j}U_{i,j-1} \tag{46}$$

where

$$\begin{aligned}\alpha_{i,j} &= \left[\frac{-l_{y_j}k11_{i+\frac{1}{2}}}{h_{y_j}h_{x_i}l_{x_i}}\right],\quad \beta_{i,j} = \left[\frac{-l_{x_i}k22_{j+\frac{1}{2}}}{h_{y_j}l_{y_j}h_{x_i}}\right],\quad \Gamma_{i,j} = \left[\frac{-l_{y_j}k11_{i-\frac{1}{2},j}}{l_{x_i}h_{x_{i-1}}h_{y_j}}\right]\\ \gamma_{i,j} &= \left[\frac{l_{y_j}k11_{i+\frac{1}{2}}}{h_{x_i}h_{y_j}l_{x_i}} + \frac{l_{y_j}k11_{i-\frac{1}{2}}}{l_{x_i}h_{x_{i-1}}h_{y_j}} + \frac{l_{x_i}k22_{j+\frac{1}{2}}}{h_{y_i}l_{y_j}h_{x_i}} + \frac{l_{x_i}k22_{j-\frac{1}{2}}}{l_{y_i}h_{y_{i-1}}h_{x_i}}\right],\quad \delta_{i,j} = \left[\frac{-l_{x_i}k22_{j-\frac{1}{2}}}{h_{y_j}h_{y_{j-1}}h_{x_i}}\right].\end{aligned} \tag{47}$$

Also from (40) we have that

$$\begin{aligned}-\nabla\cdot(\mathbf{K}_2\nabla u + \mathbf{b}u) &= -\left[\nabla_x(k_{12}\nabla_y u) + \nabla_y(k_{21}\nabla_x u) + \nabla_x(b_1 x u) + \nabla_y(b_2 y u)\right]\\ &= -\left[(k_{12}+k_{21})\nabla_{xy}u + (\frac{1}{2}\rho\sigma_1\sigma_2 x + b_1 x)\nabla_x u + (\frac{1}{2}\rho\sigma_1\sigma_2 y + b_2 y)\nabla_y u + (b_1+b_2)u\right],\end{aligned} \tag{48}$$

where $\nabla_x = \dfrac{\partial}{\partial x}$, $\nabla_y = \dfrac{\partial}{\partial y}$ and $\nabla_{xy} = \dfrac{\partial^2}{\partial x\partial y}$.

Applying the central difference to the mixed diffusion term, and the first order upwind finite difference method convection term of (48), we have that

$$(k_{12}+k_{21})\nabla_{xy}u \approx (k_{12}+k_{21})_{i,j}\left[\frac{U_{i+1,j+1} - U_{i-1,j+1} - U_{i+1,j-1} + U_{i-1,j-1}}{4h_{x_i}h_{y_j}}\right], \tag{49}$$

$$\left(\frac{1}{2}\rho\sigma_1\sigma_2 + b_1\right)x\nabla_x u \approx \left(r - \sigma_1^2\right)\left[\frac{x_{i+1/2}U_{i+1,j} - x_{i-1/2}U_{i,j}}{h_{x_i}}\right], \tag{50}$$

and

$$\left(\frac{1}{2}\rho\sigma_1\sigma_2 + b_2\right)y\nabla_y u \approx \left(r - \sigma_2^2\right)\left[\frac{y_{j+1/2}U_{i,j+1} - y_{j-1/2}U_{i,j}}{h_{y_j}}\right]. \tag{51}$$

To simplify our scheme, we assume without loss of generality that $\sigma_1^2 \le r$ and $\sigma_2^2 \le r$, and therefore

$$\begin{aligned}-\nabla\cdot(K_2\nabla u + \mathbf{b}u) + cu \approx &-(k_{12}+k_{21})_{i,j}\left[\frac{U_{i+1,j+1} - U_{i-1,j+1} - U_{i+1,j-1} + U_{i-1,j-1}}{4h_x h_y}\right]\\ &- \left(r-\sigma_1^2\right)\left[\frac{x_{i+1/2}U_{i+1,j} - x_{i-1/2}U_{i,j}}{h_{x_i}}\right] - \left(r-\sigma_2^2\right)\left[\frac{y_{j+1/2}U_{i,j+1} - y_{j-1/2}U_{i,j}}{h_{y_j}}\right] + rU_{i,j}.\end{aligned} \tag{52}$$

Then we have that,

$$\begin{aligned}\widehat{\mathcal{B}}_h U_h[z_{i,j}] = &-\frac{(k_{12}+k_{21})_{i,j}}{4h_{x_i}h_{y_j}}U_{i+1,j+1} + \frac{(k_{12}+k_{21})_{i,j}}{4h_x h_{y_j}}U_{i-1,j+1} + \frac{(k_{12}+k_{21})_{i,j}}{4h_{x_i}h_{y_j}}U_{i+1,j-1}\\ &-\frac{(k_{12}+k_{21})_{i,j}}{4h_{x_i}h_{y_j}}U_{i-1,j-1} + \left[\left(\frac{\left(r-\sigma_1^2\right)x_{i-1/2}}{h_{x_i}}\right) + \left(\frac{\left(r-\sigma_2^2\right)y_{j-1/2}}{h_{y_j}}\right) + r\right]U_{i,j}\\ &+\left(\frac{\left(r-\sigma_1^2\right)x_{i+1/2}}{h_{x_i}}\right)U_{i+1,j} + \left(\frac{\left(r-\sigma_2^2\right)y_{j+1/2}}{h_{y_j}}\right)U_{i,j+1}\end{aligned} \tag{53}$$

or

$$\widehat{\mathcal{B}}_h U_h[z_{i,j}] = \Pi_{i,j}U_{i+1,j+1} + \Lambda_{i,j}U_{i-1,j+1} + \Upsilon_{i,j}U_{i+1,j-1} + \eta_{i,j}U_{i-1,j-1} + \chi_{i,j}U_{i,j} + \zeta_{i,j}U_{i+1,j} + \varepsilon_{i,j}U_{i,j+1} \tag{54}$$

where

$$\begin{aligned}\Pi_{i,j} = -\frac{(k_{12}+k_{21})_{i,j}}{4h_{x_i}h_{y_j}},\ \Lambda_{i,j} = \frac{(k_{12}+k_{21})_{i,j}}{4h_{x_i}h_{y_j}},\ \Upsilon_{i,j} = \frac{(k_{12}+k_{21})_{i,j}}{4h_{x_i}h_{y_j}},\ \eta_{i,j} = -\frac{(k_{12}+k_{21})_{i,j}}{4h_{x_i}h_{y_j}},\\ \chi_{i,j} = -\left[\frac{1}{h_{x_i}}\left(\left(r-\sigma_1^2\right)x_i\right) + \frac{1}{h_{y_j}}\left(\left(r-\sigma_2^2\right)y_j\right) - r\right],\ \zeta_{i,j} = \frac{1}{h_{x_i}}\left(\left(r-\sigma_1^2\right)x_i\right),\\ \varepsilon_{i,j} = \frac{1}{h_{y_j}}\left(\left(r-\sigma_2^2\right)y_j\right)\end{aligned} \tag{55}$$

Now from (46) and (54), we have that

$$\begin{aligned}\widehat{\mathcal{C}}_h U_h[z_{i,j}] = \widehat{\mathcal{A}}_h U_h[z_{i,j}] + \widehat{\mathcal{B}}_h U_h[z_{i,j}] = \Pi_{i,j}U_{i+1,j+1} + \Lambda_{i,j}U_{i-1,j+1} + \Upsilon_{i,j}U_{i+1,j-1} + \eta_{i,j}U_{i-1,j-1}\\ +(\gamma_{i,j}+\chi_{i,j})U_{i,j} + (\alpha_{i,j}+\zeta_{i,j})U_{i+1,j} + (\beta_{i,j}+\varepsilon_{i,j})U_{i,j+1} + \Gamma_{i,j}U_{i-1,j} + \delta_{i,j}U_{i,j-1}\end{aligned} \tag{56}$$

for all $i = 1, 2, \ldots, N_x$ and $j = 1, 2, \ldots, N_y$.

Now using the transformation $t = T - t$, we have

$$\begin{cases} -\dfrac{dU_h}{dt} + \widehat{\mathcal{C}}_h U_h + \lambda\left[U_h^* - U_h\right]_+^{1/k} = f_h(t), \quad \forall t \in [0,T],\\ U_h(0) = U_h^*\end{cases} \tag{57}$$

3.4. Fitted mimetic finite difference scheme

The Black–Scholes differential operator is known to be degenerate towards the boundary and hence special techniques are required to handle the degeneracy [4,12,23]. In [12,23], the authors proposed a so-called fitted scheme to tackle the degeneracy of the PDE. In this section near $x = 0$ $(i = 1)$ and $y = 0$ $(j = 1)$, the sum of the diffusion and convection flux is approximated using the fitted scheme. Far from $x = 0$ $(i > 1)$ and $y = 0$ $(j > 1)$ however, the diffusion flux and convection flux will be approximated as in the previous section using respectively, the standard mimetic finite difference and the upwind finite difference method. This combination will yield our novel scheme called the fitted mimetic finite difference scheme. As the case $(i > 1, j > 1)$ is already covered in the previous section, we will only focus on the cases $(i, j = 1)$, $(i = 1, j > 1)$ and $(i > 1, j = 1)$.

3.4.1. Case I $(i, j = 1)$

We need to approximate the flux at $x_{1/2}$ and $y_{1/2}$ with the fitted finite volume method to handle the degeneracy of the Black–Scholes differential operator. Indeed, to find a new approximation at $(\mathcal{D}W)_{1,1}$, we require the fluxes at $(x_{\frac{1}{2}}, y_1)$, $(x_{\frac{3}{2}}, y_1)$ and $(x_1, y_{\frac{1}{2}})$, $(x_1, y_{\frac{3}{2}})$, i.e. $(\mathcal{G}U)_{\frac{1}{2},1}$, $(\mathcal{G}U)_{\frac{3}{2},1}$, $(\mathcal{G}U)_{1,\frac{1}{2}}$ and $(\mathcal{G}U)_{1,\frac{3}{2}}$ respectively. Now integrating (40) across $\mathcal{R}_{1,1} = [x_{\frac{1}{2}}, x_{\frac{3}{2}}] \times [y_{\frac{1}{2}}, y_{\frac{3}{2}}]$ we have

$$\begin{aligned}-\int_{x_{\frac{1}{2}}}^{x_{\frac{3}{2}}}\int_{y_{\frac{1}{2}}}^{y_{\frac{3}{2}}}\frac{\partial u}{\partial t}dxdy &- \int_{x_{\frac{1}{2}}}^{x_{\frac{3}{2}}}\int_{y_{\frac{1}{2}}}^{y_{\frac{3}{2}}}\nabla_x\cdot\left(k_{11}\nabla_x u + k_{12}\nabla_y u + b_1 xu\right)dxdy\\ &- \int_{x_{\frac{1}{2}}}^{x_{\frac{3}{2}}}\int_{y_{\frac{1}{2}}}^{y_{\frac{3}{2}}}\nabla_y\cdot\left(k_{21}\nabla_x u + k_{22}\nabla_y u + b_2 yu\right)dxdy\\ &+ \int_{x_{\frac{1}{2}}}^{x_{\frac{3}{2}}}\int_{y_{\frac{1}{2}}}^{y_{\frac{3}{2}}}\left[cu + \lambda[u^* - u]_+^{1/k} - f(t)\right]dxdy = 0.\end{aligned} \tag{58}$$

and using the midpoint rule, to approximate the first and last terms of (58), we obtain

$$
\begin{aligned}
&-R_{1,1}\frac{dU_{1,1}}{dt} - \int_{x_{\frac{1}{2}}}^{x_{\frac{3}{2}}}\int_{y_{\frac{1}{2}}}^{y_{\frac{3}{2}}} \nabla_x\cdot\left(k_{11}\nabla_x u + k_{12}\nabla_y u + b_1 xu\right)dxdy \\
&- \int_{x_{\frac{1}{2}}}^{x_{\frac{3}{2}}}\int_{y_{\frac{1}{2}}}^{y_{\frac{3}{2}}} \nabla_y\cdot\left(k_{21}\nabla_x u + k_{22}\nabla_y u + b_2 yu\right)dxdy \\
&+R_{1,1}[cU_{1,1} + \lambda[U^*_{1,1} - U_{1,1}]_+^{1/k} - f_{1,1}(t)] = 0,
\end{aligned} \tag{59}
$$

where $R_{1,1} = l_{x_1}l_{y_1}$ is the area of a control volume around the point (x_1, y_1), with $U_{x_1,y_1} = U_{1,1}$, $U^*_{x_1,y_1} = U^*_{1,1}$ and $f_{x_1,y_1} = f_{1,1}$. Let us define the following

$$
\Phi(u) := \frac{1}{2}\sigma_1^2 x\nabla_x u + (r - \sigma_1^2 - \rho\sigma_1\sigma_2)u = \mathsf{a}_1 x\nabla_x u + b_1 u \tag{60}
$$

and

$$
\Psi(u) := \frac{1}{2}\sigma_2^2 y\nabla_y u + (r - \sigma_2^2 - \rho\sigma_1\sigma_2)u = \mathsf{a}_2 y\nabla_y u + b_2 u, \tag{61}
$$

where $\mathsf{a}_1 = \frac{1}{2}\sigma_1^2$, $\mathsf{a}_2 = \frac{1}{2}\sigma_2^2$, and b_1, b_2 are as already defined. Then the second term of (59) can be approximated by

$$
\begin{aligned}
-\int_{x_{\frac{1}{2}}}^{x_{\frac{3}{2}}}\int_{y_{\frac{1}{2}}}^{y_{\frac{3}{2}}} \nabla_x\cdot\left(k_{11}\nabla_x u + k_{12}\nabla_y u + b_1 xu\right)dxdy &= -\int_{x_{\frac{1}{2}}}^{x_{\frac{3}{2}}}\int_{y_{\frac{1}{2}}}^{y_{\frac{3}{2}}} \nabla_x\cdot\left(x\Phi(u) + k_{12}\nabla_y u\right)dxdy \\
&\approx l_{y_1}\,[x\Phi(u) + k_{12}\nabla_y u]\Big|_{(x_{\frac{1}{2}},y_1)}^{(x_{\frac{3}{2}},y_1)},
\end{aligned} \tag{62}
$$

and the third term of (59) can be approximated by

$$
\begin{aligned}
-\int_{x_{\frac{1}{2}}}^{x_{\frac{3}{2}}}\int_{y_{\frac{1}{2}}}^{y_{\frac{3}{2}}} \nabla_y\cdot\left(k_{21}\nabla_x u + k_{22}\nabla_y u + b_2 yu\right)dxdy &= -\int_{x_{\frac{1}{2}}}^{x_{\frac{3}{2}}}\int_{y_{\frac{1}{2}}}^{y_{\frac{3}{2}}} \nabla_y\cdot\left(y\Psi(u) + k_{21}\nabla_x u\right)dxdy \\
&\approx l_{x_1}\,[y\Psi(u) + k_{21}\nabla_x u]\Big|_{(x_1,y_{\frac{1}{2}})}^{(x_1,y_{\frac{3}{2}})}.
\end{aligned} \tag{63}
$$

Now we have

$$
[x\Phi(u)]_{(x_{\frac{1}{2}},y_1)}^{(x_{\frac{3}{2}},y_1)} = x_{3/2}\Phi_{\frac{3}{2},1}(u) - x_{1/2}\Phi_{\frac{1}{2},1}(u). \tag{64}
$$

Note here that the problem is not at $(x_{3/2}, y_1)$ and hence using (38), $x_{3/2}\Phi(u)|_{x_{3/2},y_1}$ can be approximated as

$$
\begin{aligned}
x_{3/2}\Phi(u)|_{x_{3/2},y_1} &\approx (-\mathcal{G}U)_{3/2,1} + b_1 x_{3/2}U_{1,1} \\
&= \left[\frac{l_{y_1}k_{11_{\frac{3}{2}}}}{h_{x_1}h_{y_1}}\right]U_{2,1} + \left[b_1 x_{3/2} - \frac{l_{y_1}k_{11_{\frac{3}{2}}}}{h_{x_1}h_{y_1}}\right]U_{1,1}.
\end{aligned}
$$

Let us now consider $x_{1/2}\Phi(u)|_{x_{1/2},y_1}$ using the fitted technique [12,23]. We consider the following two-point boundary value problem:

$$
(\mathsf{a}_1 x\nabla_x v + b_1 v)' = C_1, \quad x \in (0, x_1) \tag{65}
$$

$$
v(0, y_1) = U_{0,1}, \quad v(x_1, y_1) = U_{1,1}, \tag{66}
$$

where C_1 is an unknown constant to be determined. Integrating (65) once, we have that

$$
\mathsf{a}_1 x\nabla_x v + b_1 v = C_1 x + C_2
$$

Now, using the condition $v(0, y_1) = U_{0,1}$, we have that $C_2 = b_1 U_{0,1}$ and hence

$$
\Phi_0(u) := \mathsf{a}_1 x\nabla_x v + b_1 v = C_1 x + b_1 U_{0,1}. \tag{67}
$$

Following [12], we have

$$
(\Phi(v))|_{x_{1/2},y_1} = (\mathsf{a}_1 x\nabla_x v + b_1 v)_{x_{1/2},1} = \frac{1}{2}[(\mathsf{a}_1 + b_1)U_{1,1} - (\mathsf{a}_1 - b_1)U_{0,1}]. \tag{68}
$$

Then (67) reduces to

$$
v = (U_{1,1} - U_{0,1})x/x_1, \quad x \in [0, x_1]. \tag{69}
$$

Then from (64) and (68), we have that

$$[x\Phi(u)]_{(x_{\frac{1}{2}},y_1)}^{(x_{\frac{3}{2}},y_1)} \approx \left[\frac{l_{y_1}k_{11_{\frac{3}{2}}}}{h_{x_1}h_{y_1}}\right]U_{2,1} + \left[b_1x_{3/2} - \frac{l_{y_1}k_{11_{\frac{3}{2}}}}{h_{x_1}h_{y_1}}\right]U_{1,1} - \frac{x_{1/2}}{2}[(\mathsf{a}_1+b_1)U_{1,1} - (\mathsf{a}_1-b_1)U_{0,1}]. \tag{70}$$

We follow a similar argument as before and establish that (63), can be approximated as

$$[y\Psi(u)]_{(x_1,y_{\frac{1}{2}})}^{(x_1,y_{\frac{3}{2}})} \approx \left[\frac{l_{x_1}k_{22_1}}{h_{y_1}h_{x_1}}\right]U_{1,2} + \left[b_2y_{3/2} - \frac{l_{x_1}k_{22_1}}{h_{y_1}h_{x_1}}\right]U_{1,1} - \frac{y_{1/2}}{2}[(\mathsf{a}_2+b_2)U_{1,1} - (\mathsf{a}_2-b_2)U_{1,0}]. \tag{71}$$

Remember that from (59), we have

$$\begin{aligned}&-\nabla_x\cdot\big(\Phi(u)+k_{12}\nabla_y u\big) - \nabla_y\cdot(\Psi(u)+k_{21}\nabla_x u) + cu\\ &= -\mathbf{D}\big[\big(\Phi(u)+k_{12}\nabla_y u\big) + (\Psi(u)+k_{21}\nabla_x u)\big] + cu.\end{aligned} \tag{72}$$

Then considering by definition that $\mathbf{D}$ is approximated by $\mathcal{D}$, we obtain

$$\begin{aligned}&\big[-\nabla_x\cdot\big(\Phi(u)+k_{12}\nabla_y u\big) - \nabla_y\cdot(\Psi(u)+k_{21}\nabla_x u) + cu\big]\,|x_1,y_1 \approx\\ &\frac{-\left(x_{3/2}\Phi_{\frac{3}{2},1}(u) - \frac{x_{\frac{1}{2}}}{2}[(\mathsf{a}_1+b_1)U_{1,1} - (\mathsf{a}_1-b_1)U_{0,1}]\right)}{l_{x_1}} + cU_{1,1}\\ -k_{12_{1,1}}&\frac{\big[U_{2,2}-U_{2,0}-U_{0,2}+U_{0,0}\big]}{2h_{x_1}h_{y_1}} - \frac{\left(y_{3/2}\Psi_{1,\frac{3}{2}}(u) - \frac{y_{\frac{1}{2}}}{2}[(\mathsf{a}_2+b_2)U_{1,1} - (\mathsf{a}_2-b_2)U_{1,0}]\right)}{l_{y_1}},\\ =&\frac{-\left(\left[\frac{l_{y_1}k_{11_{\frac{3}{2}}}}{h_{y_1}}\right]\frac{U_{2,1}-U_{1,1}}{h_{x_1}} - \frac{x_{\frac{1}{2}}}{2}[(\mathsf{a}_1+b_1)U_{1,1} - (\mathsf{a}_1-b_1)U_{0,1}]\right)}{l_{x_1}} - \left[\frac{k_{12_{1,1}}}{2h_{x_1}h_{y_1}}\right]\big[U_{2,2}-U_{2,0}\big]\\ -\left[\frac{k_{12_{1,1}}}{2h_{x_1}h_{y_1}}\right]&\big[U_{0,0}-U_{0,2}\big] - \frac{\left(\frac{l_{x_1}k_{22_{\frac{3}{2}}}}{h_{x_1}}\frac{U_{1,2}-U_{1,1}}{h_{y_1}} - \frac{y_{\frac{1}{2}}}{2}[(\mathsf{a}_2+b_2)U_{1,1} - (\mathsf{a}_2-b_2)U_{1,0}]\right)}{l_{y_1}} + cU_{1,1},\end{aligned} \tag{73}$$

where $U_{1,0}, U_{2,0}, U_{0,2}, U_{0,1}$ and $U_{0,0}$ are solutions obtained from the 1D problem. Now remember that $z_{i,j} = (i-1)N_x + j$ for $U_H = (U_{1,1}, U_{1,2}, \ldots, U_{1,N_y}, \ldots, U_{N_x,1}, U_{N_x,2}, \ldots, U_{N_x,N_y})^T$,

Then have that

$$\begin{aligned}C_HU_H[z_{1,1}] = &-\left[\frac{k_{12_{1,1}}}{2h_{x_1}h_{y_1}}\right]U_{2,2} - \left[\frac{l_{y_1}k_{11_{\frac{3}{2}}}}{h_{x_1}l_{x_1}h_{y_1}}\right]U_{2,1} - \left[\frac{l_{x_1}k_{22_{\frac{3}{2}}}}{l_{y_1}h_{x_1}h_{y_1}}\right]U_{1,2}\\ &+\left[\frac{l_{y_1}k_{11_{\frac{3}{2}}}}{h_{x_1}l_{x_1}h_{y_1}} + \frac{l_{x_1}k_{22_{\frac{3}{2}}}}{l_{y_1}h_{x_1}h_{y_1}} + \frac{x_{\frac{1}{2}}}{2l_{x_1}}(\mathsf{a}_1+b_1) + \frac{y_{\frac{1}{2}}}{2l_{y_1}}(\mathsf{a}_2+b_2) + c\right]U_{1,1}.\end{aligned} \tag{74}$$

3.4.2. Case II ($i = 1, j > 1$)

Again, we approximate the flux along $x_{1/2}$ and $y_j, j > 1$ with the fitted finite volume method to handle the degeneracy. The integrating (40) across $\mathcal{R}_{1,j} = [x_{\frac{1}{2}}, x_{\frac{3}{2}}] \times [y_{j-\frac{1}{2}}, y_{j+\frac{1}{2}}]$, and following a similar argument as is case 1, we have

$$\begin{aligned}&-R_{1,j}\frac{dU_{1,j}}{dt} - \int_{x_{\frac{1}{2}}}^{x_{\frac{3}{2}}}\int_{y_{j-\frac{1}{2}}}^{y_{j+\frac{1}{2}}}\nabla_x\cdot\big(k_{11}\nabla_x u + k_{12}\nabla_y u + b_1xu\big)\,dxdy\\ &-\int_{x_{\frac{1}{2}}}^{x_{\frac{3}{2}}}\int_{y_{j-\frac{1}{2}}}^{y_{j+\frac{1}{2}}}\nabla_y\cdot\big(k_{21}\nabla_x u + k_{22}\nabla_y u + b_2yu\big)\,dxdy\\ &+R_{1,j}[cU_{1,j} + \lambda[U_{1,j}^* - U_{1,j}]_+^{1/k} - f_{1,j}(t)] = 0,\end{aligned} \tag{75}$$

where $R_{1,j} = l_{x_1}l_{y_j}$ is the area of a control volume around the point (x_1, y_j), $j > 1$. We approximate the second and third terms of (75) by

$$-\int_{x_{\frac{1}{2}}}^{x_{\frac{3}{2}}}\int_{y_{j-\frac{1}{2}}}^{y_{j+\frac{1}{2}}}\nabla_x\cdot\big(k_{11}\nabla_x u + k_{12}\nabla_y u + b_1xu\big)\,dxdy \approx l_{y_1}\,[x\Phi(u) + k_{12}\nabla_y u]\Big|_{(x_{\frac{1}{2}},y_j)}^{(x_{\frac{3}{2}},y_j)}, \tag{76}$$

and

$$-\int_{x_{\frac{1}{2}}}^{x_{\frac{3}{2}}}\int_{y_{\frac{1}{2}}}^{y_{\frac{3}{2}}} \nabla_y \cdot \left(k_{21}\nabla_x u + k_{22}\nabla_y u + b_2 y u\right) dxdy \approx l_{x_1}\left[y\Psi(u) + k_{21}\nabla_x u\right]\Big|_{(x_1,y_{j-\frac{1}{2}})}^{(x_1,y_{j+\frac{1}{2}})}. \tag{77}$$

Note that our focus here will be to apply the fitted scheme to (76). The standard mimetic, central difference and the first order upwind will be used to approximate the terms of (77).

Recall that

$$[x\Phi(u)]_{(x_{\frac{1}{2}},y_j)}^{(x_{\frac{3}{2}},y_j)} = x_{3/2}\Phi_{\frac{3}{2},j}(u) - x_{1/2}\Phi_{\frac{1}{2},j}(u). \tag{78}$$

and hence using (38), $x_{3/2}\Phi(u)|_{x_{3/2},y_j}$ can be approximated as

$$\begin{aligned} x_{3/2}\Phi(u)|_{x_{3/2},y_1} &\approx (-\mathcal{G}U)_{3/2,j} + b_1 x_{3/2} U_{1,j} \\ &= \left[\frac{l_{y_j} k_{11_{\frac{3}{2}}}}{h_{y_j} h_{x_1}}\right] U_{2,j} + \left[b_1 x_{3/2} - \frac{l_{y_j} k_{11_{\frac{3}{2}}}}{h_{y_j} h_{x_1}}\right] U_{1,j}. \end{aligned}$$

To find the approximation for $x_{1/2}\Phi(u)|_{x_{1/2},y_j}$ using the fitted technique, we consider again the following two-point boundary value problem:

$$(\mathsf{a}_1 x\nabla_x v + b_1 v)' = C_1, \quad (x,y) \in (0,x_1)\times(0,Y) \tag{79}$$

$$v(0,y_j) = U_{0,j}, \quad v(x_1,y_j) = U_{1,j}, \tag{80}$$

where C_1 is an unknown constant to be determined. Then following the arguments [12], we have

$$(\Phi(v))|_{x_{1/2},y_j} = (\mathsf{a}x\nabla_x v + \mathsf{b}v)_{x_{1/2},j} = \frac{1}{2}[(\mathsf{a}_1 + b_1)U_{1,j} - (\mathsf{a}_1 - b_1)U_{0,j}], \tag{81}$$

Again following that the divergent operator $\mathbf{D}$ is approximated by $\mathcal{D}$, we can approximate the flux in (75)

$$\begin{aligned} \mathbf{D}\left[\Phi(u) + \Psi(u)\right]|_{x_1,y_j} \approx &-\frac{1}{l_{x_1}}\left(x_{3/2}\Phi(u)|_{\frac{3}{2},j} - \frac{x_{\frac{1}{2}}}{2}[(\mathsf{a}_1 + b_1)U_{1,j} - (\mathsf{a}_1 - b_1)U_{0,j}]\right) \\ &-\frac{1}{l_{y_j}}\left((\mathcal{G}U)_{1,j+\frac{1}{2}} - (\mathcal{G}U)_{1,j-\frac{1}{2}} + b_2 y_{j+\frac{1}{2}} U_{i,j+1} - b_2 y_{j-\frac{1}{2}} U_{i,j}\right) \end{aligned} \tag{82}$$

and

$$-\nabla\cdot\left[K_2\nabla u\right]|_{x_1,y_j} \approx -\left[k_{21_{1,j}}\frac{U_{2,j+1} - U_{0,j+1} + U_{2,j-1} + U_{0,j-1}}{2h_{x_1}h_{y_j}}\right] \tag{83}$$

$$\begin{aligned} &\left[\mathbf{D}\left[\Phi(u) + \Psi(u)\right]|_{x_1,y_j}\right] - \nabla\cdot\left[K_2\nabla u\right]\Big|_{x_1,y_j} \approx \\ &-\frac{\left(\left[\frac{l_{x_1}k_{22_{j+\frac{1}{2}}}}{h_{x_1}}\right]\frac{U_{1,j+1} - U_{1,j}}{h_{y_j}} - \left[\frac{l_{x_1}k_{22_{j-\frac{1}{2}}}}{h_{x_1}}\right]\frac{U_{1,j} - U_{1,j-1}}{h_{y_{j-1}}}\right)}{l_{y_j}} + cU_{1,j} \\ &-\frac{\left(b_2 y_{j+\frac{1}{2}} U_{i,j+1} - b_2 y_{j-\frac{1}{2}} U_{i,j}\right)}{l_{y_j}} - \left[k_{21_{1,j}}\frac{U_{2,j+1} - U_{0,j+1} + U_{2,j-1} + U_{0,j-1}}{2h_{x_1}h_{y_j}}\right]. \end{aligned} \tag{84}$$

Then we have

$$\begin{aligned} C_H U_H[z_{1,j}] = &-\left[\frac{k_{12_{1,j}}}{2h_{x_1}h_{y_j}}\right]U_{2,j+1} - \left[\frac{l_{y_j}k_{11_{\frac{3}{2}}}}{h_{y_j}h_{x_1}l_{x_1}}\right]U_{2,j} - \left[\frac{k_{12_{1,j}}}{2h_{x_1}h_{y_j}}\right]U_{2,j-1} \\ &-\left[\frac{l_{x_1}k_{22_{j+\frac{1}{2}}}}{h_{x_1}h_{y_j}l_{y_j}} + \frac{b_2 y_{j+\frac{1}{2}}}{l_{y_j}}\right]U_{1,j+1} + \left[\frac{l_{x_1}k_{22_{j-\frac{1}{2}}}}{l_{y_j}h_{y_{j-1}}h_{x_1}}\right]U_{1,j-1} \\ &+\left[\frac{l_{y_j}k_{11_{\frac{3}{2}}}}{h_{y_j}h_{x_1}l_{x_1}} + \frac{l_{x_1}k_{22_{j+\frac{1}{2}}}}{h_{x_1}h_{y_j}l_{y_j}} + \frac{l_{x_1}k_{22_{j-\frac{1}{2}}}}{h_{x_1}h_{y_{j-1}}l_{y_j}} + \frac{x_{\frac{1}{2}}}{2l_{x_1}}(\mathsf{a}_1 + b_1) + \frac{b_2 y_{j-\frac{1}{2}}}{l_{y_j}} + c\right]U_{1,j}. \end{aligned} \tag{85}$$

3.4.3. Case III ($i > 1, j = 1$)

This case follows similarly to the previous case. Hence we have that

$$\begin{aligned} C_H U_H[z_{i,1}] = &-\left[\frac{k12_{i,1}}{2h_{x_i}h_{y_1}}\right]U_{i+1,2} - \left[\frac{l_{x_i}k22_{\frac{3}{2}}}{h_{y_1}h_{x_i}l_{y_1}}\right]U_{i,2} - \left[\frac{k12_{i,1}}{2h_{x_i}h_{y_1}}\right]U_{i-1,2} \\ &- \left[\frac{l_{y_1}k11_{i+\frac{1}{2}}}{h_{y_1}h_{x_i}l_{x_i}} + \frac{b_1 x_{i+\frac{1}{2}}}{l_{x_i}}\right]U_{i+1,1} + \left[\frac{l_{y_1}k11_{i-\frac{1}{2}}}{l_{x_i}h_{x_{i-1}}h_{y_1}}\right]U_{i-1,1} \\ &+ \left[\frac{l_{x_i}k22_{\frac{3}{2}}}{h_{x_i}h_{y_1}l_{y_1}} + \frac{l_{y_1}k11_{i+\frac{1}{2}}}{h_{y_1}h_{x_i}l_{x_i}} + \frac{l_{y_1}k11_{i-\frac{1}{2}}}{h_{y_1}h_{x_{i-1}}l_{x_i}} + \frac{y_{\frac{1}{2}}}{2l_{y_1}}(a_2+b_2) + \frac{b_1 x_{i-\frac{1}{2}}}{l_{x_i}} + c\right]U_{i,1}. \end{aligned} \tag{86}$$

Now combining the mimetic approximation of (57) at $(x_i, y_j), i > 1, j > 1$, with (74), (85) and (86), yields our novel scheme called the fitted mimetic finite difference method. Therefore for

$$U_H = (U_{1,1}, U_{1,2}, \ldots, U_{1,N_y}, \ldots, U_{N_x,1}, U_{N_x,2}, \ldots, U_{N_x,N_y})^T,$$

using the transformation $t = T - t$, we need to solve in the case of the fitted mimetic method the following system,

$$\begin{cases} \dfrac{dU_H}{dt} + \mathcal{C}_H U_H + F(U_H, t) = 0, \quad t \in [0, T], \\ U_H(0) = U_H^* \\ F(U_H, t) = \lambda\left[U_H^* - U_H\right]_+^{1/k} - f_H(t), \end{cases} \tag{87}$$

where

$$\begin{cases} C_H U_H[z_{1,1}], \quad \text{is as given in (74)} \\ C_H U_H[z_{1,j}], \ j > 1, \quad \text{is as given in (85)} \\ C_H U_H[z_{i,1}], \ i > 1, \quad \text{is as given in (86)} \\ C_H U_H[z_{i,j}] = \widehat{C}_h U_h[z_{i,j}], \ i > 1, j > 1 \end{cases} \tag{88}$$

with $z_{i,j} = (i-1) \times N_x + j$.

3.5. Time discretization using standard implicit schemes

We subdivide the time interval $[0, T]$ in M subdivisions. That is, $0 = t_0 < t_1 < \cdots < t_M = T$, such that $\Delta t = t_{m+1} - t_m$, for $m = \{0, 1, \ldots, M\}$. We adopt the stable time discretization method mostly used, that is the Euler-θ-methods for (57) and (87) representing the semi-discrete solutions for the standard mimetic finite difference method and the fitted mimetic finite difference method, respectively, and is given by

$$\begin{cases} \dfrac{U_h^{m+1} - U_h^m}{\Delta t} = \theta\left(\widehat{C}_h U_h^{m+1} + F(U_h^{m+1}, t_{m+1})\right) + (1-\theta)\left(\widehat{C}_h U_h^m + F(U_h^m, t_m)\right) \\ U_h(0) = U_h^*, \qquad 0 < \theta \le 1, \end{cases} \tag{89}$$

and

$$\begin{cases} \dfrac{U_H^{m+1} - U_H^m}{\Delta t} = \theta\left(C_H U_H^{m+1} + F(U_H^{m+1}, t_{m+1})\right) + (1-\theta)\left(C_H U_H^m + F(U_H^m, t_m)\right) \\ U_H(0) = U_H^*, \qquad 0 < \theta \le 1, \end{cases} \tag{90}$$

The scheme (89) is order 2 in time when $\theta = 1/2$ and order 1 if $\theta \neq 1/2$.

4. Numerical tests

In this section, we run numerical simulations on a 8 GB 1600 MHz DDR3, Macbook Pro (13-inch, Mid 2012). We will consider two tests. The first test will be for pricing the European put option and the second test will be for pricing the American put option.

4.1. European put options

For the first test, we consider the case when the penalty parameter $\lambda = 0$ in (10). Indeed, this case corresponds to the solution of the European put option. As remarked earlier, there exits a closed form solution to the Black–Scholes PDE

Table 1
Table showing the two-dimensional L^2-relative error for the various spatial discretization methods for the European option. By fitting the data for fitted finite volume method, we found that the order of convergence in space is 0.99. This order confirms the theoretical result in [12].

N	Fitted finite volume error	Mimetic FDM error	Fitted mimetic FDM error
10×10	0.1095	0.0061	0.0056
15×15	0.0733	0.0059	0.0055
30×30	0.0369	0.0057	0.0053
50×50	0.0222	0.0057	0.0053
75×75	0.0148	0.0056	0.0052
100×100	0.0111	0.0056	0.0052

$T = 1,\ r = 0.1,\ K = 1\ X_{\max} = Y_{\max} = 4K,\ \sigma_1 = \sigma_2 = 0.2, \rho = 0.4, \alpha_1 = \alpha_2 = 0.5, \quad \Delta t = T/100.$

Table 2
Table showing CPU time (in seconds) for the various spatial discretization methods for the European option.

N	Fitted FV CPU time	Mimetic FDM CPU time	Fitted Mimetic FDM CPU time
10×10	0.751	0.744	0.326
15×15	1.314	1.126	0.583
30×30	3.211	2.699	1.951
50×50	6.944	6.733	5.492
75×75	15.211	14.944	12.749
100×100	30.013	27.110	26.271

$T = 1,\ r = 0.1,\ K = 1\ X_{\max} = Y_{\max} = 4K,\ \sigma_1 = \sigma_2 = 0.2, \alpha_1 = \alpha_2 = 0.5, \quad \Delta t = T/100.$

when the coefficients are constant, and this is given in [1] as below

$$\begin{aligned} U(s_1, s_2, K, T) = {} & Ke^{-rT}\left(1 - M(-y_1 + \sigma_1\sqrt{T}, -y_2 + \sigma_2\sqrt{T}; \rho)\right) \\ & - s_1 e^{-rT} M(y_1, d; \rho_1) - s_2 e^{-rT} M(y_2, -d; \rho_2) \end{aligned} \tag{91}$$

where

$$d = \frac{\ln(s_1/s_2) + \left(b_1 - b_2 + \frac{\sigma_1^2}{2}\right)T}{\sigma\sqrt{T}},$$

$$y_1 = \frac{\ln(s_1/K) + \left(b_1 + \frac{\sigma_1^2}{2}\right)T}{\sigma\sqrt{T}}, \quad y_2 = \frac{\ln(s_2/K) + \left(b_2 + \frac{\sigma_2^2}{2}\right)T}{\sigma\sqrt{T}},$$

$$\sigma = \sqrt{\sigma_1^2 + \sigma_2^2 - \rho\sigma_1\sigma_2}, \quad \rho_1 = \frac{\sigma_1 - \rho\sigma_2}{\sigma}, \quad \rho_2 = \frac{\sigma_2 - \rho\sigma_2}{\sigma}$$

and

$$M(a, b; \rho) = \frac{1}{2\pi\sqrt{1-\rho^2}} \int_{-\infty}^{a}\int_{-\infty}^{a} \exp\left(\frac{x^2 - 2\rho xy + y^2}{2(1-\rho^2)}\right) dxdy. \tag{92}$$

Indeed, to compute the relative error, we use the L^2-norm given by

$$Error = \frac{\sqrt{\sum_{i=1}^{N_x}\sum_{j=1}^{N_y} h_{x_i} h_{y_j} (U_{i,j} - U_{i,j}^{\text{analytic}})^2}}{\sqrt{\sum_{i=1}^{N_x}\sum_{j=1}^{N_y} h_{x_i} h_{y_j} (U_{i,j}^{\text{analytic}})^2}}, \tag{93}$$

where $U_{i,j}$ and $U_{i,j}^{\text{analytic}}$ are respectively the numerical solution and the analytical solution at (x_i, y_j) (see Fig. 2).

From Table 1, we can observe the accuracy of the mimetic methods comparing to the finite volume method. The table further shows the importance of the fitted scheme as the fitted mimetic scheme outperforms the standard mimetic scheme. Furthermore, we present the CPU timings in seconds of all the methods. From Table 2, we see that the computational timings for the methods are quite close. This is due to the fact that the matrix representation of all the methods are similar.

4.2. American put options

Since American options in general have no analytical solution even when the Black–Scholes operator has constant parameters, in our case, we choose the fitted mimetic scheme as the reference solution. Our motivation of choosing the

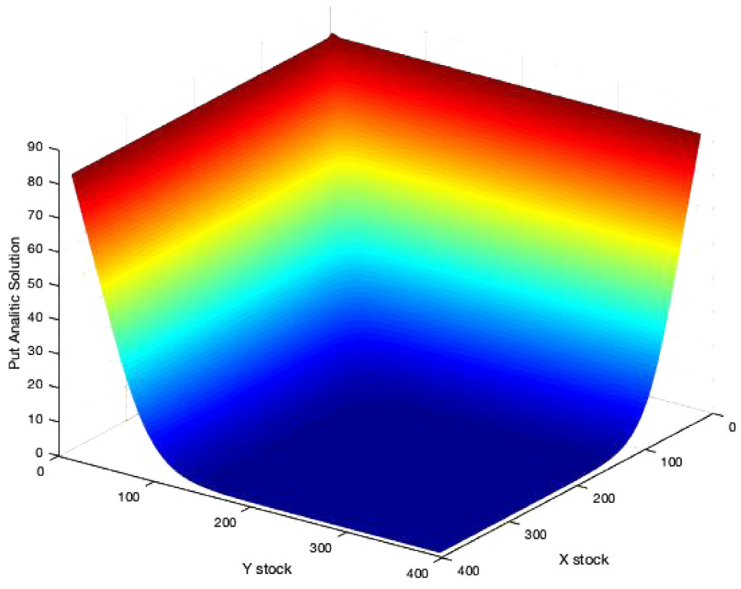

(a)

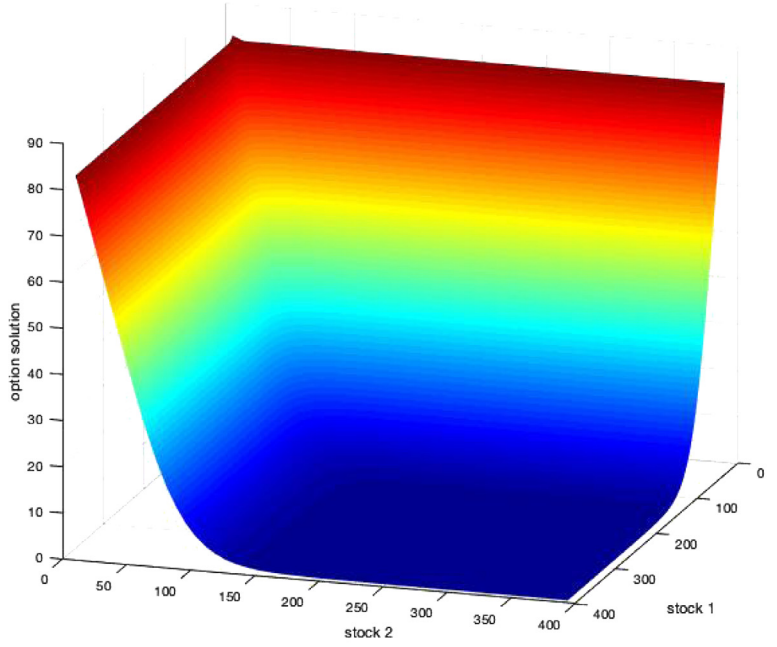

(b)

Fig. 2. The analytical solution of the European put option is given in (a) while the corresponding numerical solution based on mimetic numerical is given in (b).

fitted mimetic scheme as reference solution is based on the fact that the fitted scheme seems to be more accurate than the other schemes as we have seen in the previous test for European option. The fitted mimetic method is therefore used as an analytical solution. The relative error is computed as shown in the table below: We can observe from Table 3 that the mimetic method remain superior to the fitted finite volume method [23] for pricing American put option problem. Note that we have used the Newton method with tolerance tol$= 10^{-7}$, to solve at each iteration the non-linear full discrete equations in (89) and (90) with $\theta = 1$, with initial guess U_h^m. Remember that $[U_h^{*m} - U_h^m]_+^{1/k} = \max\left\{[U_h^{*m} - U_h^m]^{1/k}, 0\right\}$,

Table 3
This table shows the two-dimensional L^2-relative error for the various spatial discretization methods for the American put option. By fitting the data for the Mimetic method, we found that the order of convergence in space is 1.08. This order might be 2 if the second order upwinding technique [24] is used to approximate the convection term.

N	Fitted Finite Volume Error	Mimetic FDM Error
10×10	0.1428	0.0241
20×20	0.1058	0.0052
30×30	0.0711	0.0033
50×50	0.0698	0.0022
75×75	0.0592	0.0018
85×85	0.0600	0.0017
100×100	0.0570	0.0016

$T = 1,\ r = 0.1, K = 1,\ X = Y = 4K,\ \sigma_1 = \sigma_2 = 0.2,\ \rho = 0.4,\ \alpha_1 = \alpha_2 = 0.5,$ tolerance (tol) $= 10^{-7}, \epsilon = 10^{-4},\ \Delta t = T/100$, and penalty parameters: $\lambda = 100,\ k = 2$.

Table 4
This table shows the CPU timings (in seconds) for the spatial discretization methods for the American put option.

N	Fitted Finite Volume CPU time (s)	Mimetic FDM CPU time (s)
10×10	0.369	0.352
20×20	0.714	0.688
30×30	1.826	1.721
50×50	11.935	11.529
75×75	15.881	14.672
85×85	19.769	18.948
100×100	28.951	26.869

$T = 1,\ r = 0.1, K = 1,\ X = Y = 4K,\ \sigma_1 = \sigma_2 = 0.2,\ \rho = 0.4,\ \alpha_1 = \alpha_2 = 0.5,$ tolerance (tol) $= 10^{-7}, \epsilon = 10^{-4},\ \Delta t = T/100$, and penalty parameters: $\lambda = 100,\ k = 2$.

that is for $\epsilon > 0$, we have

$$[U_h^{*m} - U_h^m]_+^{1/k} = \begin{cases} [U_h^{*m} - U_h^m]^{1/k}, & \text{if } U_h^{*m} - U_h^m \geq \epsilon \\ 0, & \text{otherwise.} \end{cases} \tag{94}$$

The CPU timings of the methods are shown in the Table 4 below:

5. Conclusion

In this paper, we have provided the mimetic and fitted mimetic finite difference methods to approximate the two dimensional degenerate Black–Scholes differential operator governing option pricing. We have presented the support operator method which underlies the construction of the standard mimetic finite difference method and novel fitted mimetic finite difference method. Indeed, to handle the degeneracy of near the boundary at zero of the Black–Scholes differential operator, we have proposed the fitted scheme. The novel combined scheme (fitted mimetic finite difference method) has out-performed the standard mimetic and fitted finite volume methods when numerical experiments were conducted for European and American options.

Declaration of competing interest

Antoine Tambue reports financial support was provided by Robert–Bosch Foundation GmbH. All the authors (D.S. Attipoe and A. Tambue) of this work were supported by the Robert Bosch Stiftung through the AIMS ARETE Chair programme (Grant No 11.5.8040.0033.0).

Acknowledgments

This work was supported by the Robert Bosch Stiftung (Germany) through the AIMS ARETE Chair programme (Grant No 11.5.8040.0033.0) and the Western Norway University of Applied Sciences.

References

[1] Haug EG. The complete guide to option pricing formulas. Vol. 2. New York: McGraw-Hill; 2007.
[2] Black F, Scholes M. The pricing of options and corporate liabilities. J Polit Econ 1973;81(3):637–59.
[3] Hull J. Options, futures, and other derivatives. Englewood Cliffs: Prentice-hall; 2005.
[4] Zhang K, Wang S, Yang XQ, Teo KL. Power penalty method for a linear complementarity problem arising from American option valuation. J Optim Theory Appl 2006;129(2):227–54.

[5] Duffy Daniel J. Finite difference methods in financial engineering: a partial differential equation approach. West Sussex, England: John Wiley & Sons Ltd; 2006.
[6] Almushaira M, Chen F, Lui F. Efficient operator splitting and spectral methods for the time-space fractional Black Scholes equation. Results Appl Math 2021;10:100149.
[7] Haslinger J, Miettinen M, Panagiotopoulos DP. Finite element method for hemivariational inequalities. In: Theory, methods and applications. Dordrecht: Kluwer Academic Publishers; 1999.
[8] Zvan R, Forsyth PA, Vetzal KR. Penalty methods for American options with stochastic volatility. J Comput Appl Math 1998;91(2):199–218.
[9] Huang J, Pang J-S. Option pricing and linear complementarity. J Comput Finance 1998;2(3):31–60.
[10] Vazquez C. An upwind numerical approach for an American and European option pricing model. Appl Math Comput 1998;97(2):273–86.
[11] Attipoe DS, Tambue A. Convergence of the mimetic finite difference and fitted mimetic finite difference method for options pricing. Appl Math Comput 2021;401. http://dx.doi.org/10.1016/j.amc.2021.126060.
[12] Wang S. A novel fitted finite volume method for the Black–Scholes equation governing option pricing. IMA J Numer Anal 2004;24:699–720.
[13] Angermann L, Wang S. Convergence of a fitted finite volume method for the penalized Black–Scholes equation governing European and American option pricing. Numer Math 2007;106:1–40.
[14] Kufner A. Weighted sobolev spaces. John Wiley & Sons; 1985.
[15] Nielsen BF, Skavhaug O, Tveito A. Penalty methods for the numerical solution of American multi-asset option problems. J Comput Appl Math 2008;222(1):3–16.
[16] Hyman J, Shashkov M, Steinberg S. The numerical solution of diffusion problems in strongly heterogeneous non-isotropic materials. J Comput Phys 1997;132:130–48.
[17] Lipnikov K, Morel J, Shashkov M. Mimetic finite difference methods for diffusion equations on non-orthogonal non-conformal meshes. J Comput Phys 2004;199:589–97.
[18] Lipnikov K, Shashkov M, Svyatskiy D. The mimetic finite difference discretization of diffusion problem on unstructured polyhedral meshes. J Comput Phys 2006;211:473–91.
[19] Gyrya V, Lipnikov K. High-order mimetic finite difference method for diffusion problem on polygonal meshes. J Comput Phys 2008;227:8841–54.
[20] Winters A, Shashkov M. Support operators method for the diffusion equation in multiple materials. United States: Los Alamos National Laboratory; 2012.
[21] Shashkov M, Steinberg S. Solving diffusion equations with rough coefficients in rough grids. J Comput Phys 1996;129:383–405.
[22] Lie KA, Krogstad S, Ligaarden IS, Natvig JR, Nilsen HM, Bård Skaflestad B. Open-source matlab implementation of consistent discretisations on complex grids. Comput Geosci 2012;16(2):297–322.
[23] Huang CS, Hung CH, Wang S. A fitted finite volume method for the valuation of options on assets with stochastic volatilities. Computing 2006;77(3):297–320.
[24] Koffi RS, Tambue A. A fitted L-multi-point flux approximation method for pricing options. Comput Econ 2021. http://dx.doi.org/10.1007/s10614-021-10161-2.